

Carbonyl-Supported Coordination in Imidazolates: A Platform for Designing Porous Nickel-Based ZIFs as Heterogeneous Catalysts

Aljaž Škrjanc, Dominik Jankovič, Anton Meden, Matjaž Mazaj, Erik Svensson Grape, Martin Gazvoda, and Nataša Zabukovec Logar*

Zeolitic imidazolate frameworks (ZIFs) are a subclass of metal–organic framework that have attracted considerable attention as potential functional materials due to their high chemical stability and ease of synthesis. ZIFs are usually composed of zinc ions coordinated with imidazole linkers, with some other transition metals, such as Cu(II) and Co(II), also showing potential as ZIF-forming cations. Despite the importance of nickel in catalysis, no Ni-based ZIF with permanent porosity is yet reported. It is found that the presence and arrangement of the carbonyl functional groups on the imidazole linker play a crucial role in completing the preferred octahedral coordination of nickel, revealing a promising platform for the rational design of Ni-based ZIFs for a wide range of catalytic applications. Herein, the synthesis of the first Ni-based ZIFs is reported and their high potential as heterogeneous catalysts for Suzuki–Miyaura cross-coupling C–C bond forming reactions is demonstrated.

1. Introduction

In recent years, reticular chemistry has emerged as a significant and diverse field in materials science, with a wide range of functionalities being used in different applications.^[1–3] ZIFs, as a subclass of metal–organic frameworks (MOFs), represent one such type of reticular material. Despite significant progress and rapid expansion in the field of structure engineering, the majority of ZIFs still consist of tetrahedrally coordinated metal nodes, with zinc being the most commonly represented.^[4] To date, ZIFs with other transition metals such as Co, Cu, and Cd have also been reported.^[5] Additionally, ZIF-8 structure analogues built from Li/Al,^[6] Fe,^[7] Mn,^[8] and Mg^[9] tetrahedra are known, but are unstable in air or humid conditions.

Ni-based compounds have gained popularity as heterogeneous catalysts for various applications, including CO₂ dry reforming,^[10] olefin oligomerization,^[11,12] selective deoxygenation for biofuel production,^[13] and hydrogenation,^[14] as they present a more affordable alternative to Pd or Pt-based catalysts. Moreover, nickel compounds play an important role in energy storage and conversion systems like electrochemical capacitors,^[15] batteries,^[16] and solar cells.^[17]

The advantageous properties of nickel are further highlighted in porous MOF structures, which exhibit accessible isolated metal nodes. In recent years, Ni-containing MOFs have also been proposed as catalysts in various coupling reactions.^[18,19] Developments in this area of organic synthesis^[20] have mainly been focused on the immobilization of the established ligands from homogeneous catalysis^[21,22] onto the surface of a MOF, leading to the development of a sustainable heterogeneous nickel catalyst;^[23] and on nickel-decorated covalent organic frameworks for reactions under microwave irradiation,^[24] both of which have shown promising results in Suzuki–Miyaura coupling.

With reusability and cyclability at the forefront of potential catalyst design, the performance of the catalyst after several reaction cycles is one of the main criteria for the development of sustainable catalysts. In the case of MOFs, it mostly refers to the structural stability of the MOF catalyst under selected reaction conditions. Alternatively, MOF-based and other heterogeneous or even homogeneous (pre)catalysts can also serve as reservoirs for

A. Škrjanc, M. Mazaj, N. Zabukovec Logar
Department of Inorganic Chemistry and Technology
National Institute of Chemistry
Hajdrihova 19, Ljubljana 1001, Slovenia
E-mail: natasa.zabukovec@ki.si

A. Škrjanc, N. Zabukovec Logar
School of Science
University of Nova Gorica
Vipavska 13, Nova Gorica 5000, Slovenia

D. Jankovič, A. Meden, M. Gazvoda
Faculty of Chemistry and Chemical Technology
University of Ljubljana
Večna pot 113, Ljubljana 1001, Slovenia

E. S. Grape
Department of Materials and Environmental Chemistry
Stockholm University
Stockholm 106 91, Sweden

 The ORCID identification number(s) for the author(s) of this article can be found under <https://doi.org/10.1002/smll.202305258>

© 2023 The Authors. Small published by Wiley-VCH GmbH. This is an open access article under the terms of the Creative Commons Attribution-NonCommercial-NoDerivs License, which permits use and distribution in any medium, provided the original work is properly cited, the use is non-commercial and no modifications or adaptations are made.

DOI: 10.1002/smll.202305258

catalytically active nickel nano-species that are formed in situ in the reaction media.^[25]

Nickel, while a commonly used metal node in MOF synthesis, has to date only been used in the preparation of mixed metal (MM) ZIFs with a highest Ni/Zn ratio of 1:1, reported by Li et al.^[26] in 2014 in the MM ZIF-8 system they developed for photocatalysis and time-resolved alcohol sensing. They reported that mechanochemical attempts to produce ZIFs with a higher Ni content tended to result in the formation of individual Ni imidazolate coordination compounds and not in a 3D framework, while solvothermal synthesis produced an almost pure Zn ZIF with very low Ni content. Similar results from solvothermal synthesis were also obtained by Chen et al.^[27] with the development of Ni-ZIF-8 for ethylene dimerization with a maximum incorporated Ni amount of 0.7 w%.

While a pure nickel 2-methylimidazolate coordination polymer that forms 2D nanosheets, but lacks permanent microporosity, has been successfully utilized both in photocatalysis^[28] and as an advanced electrode material,^[29] to our knowledge no pure crystalline nickel-based crystalline ZIF-like material with a permanent porous zeolite-type framework has yet been reported.

Most initial attempts to prepare Ni-based ZIFs were usually conducted with less expensive linkers such as 2-methylimidazole and imidazole, which would result in tetrahedrally coordinated Ni²⁺. With nickel complexes known to prefer octahedral or square planar coordination,^[30] and with the latter not leading to 3D frameworks, we decided to look into linkers with functional groups that could form additional coordination bonds, thereby completing the octahedral coordination environment of Ni²⁺. A review of linkers of common ZIFs led us to speculate that the presence of an oxygen containing functional group, such as an aldehyde or ester, could stabilize the framework formation and lead to Ni based ZIFs. This hypothesis was tested using two imidazoles with an aldehyde group, that is, 2-imidazolecarboxaldehyde (Figure 1a) and 4-methyl-5-imidazolecarboxaldehyde (Figure 1b), respectively, which are commonly used in ZIF-90 and ZIF-94/ZIF-93 synthesis.

Through the appropriate selection of carbonyl-functionalized imidazole-based ligands, we have successfully designed the first pure nickel ZIFs with permanent porosity, which exhibit zeolitic RHO and SOD topologies.^[31] Both ZIFs demonstrate efficient performance as heterogeneous catalysts in the Suzuki–Miyaura C–C coupling reaction.

2. Results and Discussion

2.1. Material Synthesis and Characterization

Initial synthesis attempts with 2-imidazolecarboxaldehyde (NICS-21) were made with an ageing time of 1 day, but powder X-ray diffractograms (PXRD) analysis showed the samples to have broad peaks with some secondary phase present (Figure S2.1, Supporting Information). The synthesis time was then extended to 3 days to obtain satisfactory crystallinity and phase purity. In the course of optimizing the reaction, multiple attempts were made with changes to various parameters (Figure S2.2, Supporting Information). In all cases, higher temperatures led to the formation of nonporous, 2D, leaf-like structure previously reported for nickel with 2-methylimidazole.^[29] Since the

exact structure of the latter is not known, we cannot provide an explanation for the 2D structure formation at higher temperatures. However, it is quite common that even smaller adjustments of reaction parameters during the synthesis or after the synthesis can induce formation or structural inter-dimensional (2D/3D) transformations of ZIFs, generating various thermodynamically or kinetically stable phases.^[32,33] Variation in reagent ratios for the attempts to prepare larger crystals resulted in the formation of NICS-21, but there was also always a substantial quantity of impurities, leading us to continue the study with the initial synthesis conditions.

A product with 4-methyl-5-imidazolecarboxaldehyde (NICS-22) was prepared using a modified one-pot solvothermal synthesis at 80 °C in a capped round-bottom flask. Due to the elevated temperature, desirable crystallinity and phase purity could be obtained after 1 day.

Both frameworks' SEMs show agglomerated single phase nanocrystalline particles (Figure 1a,b).

The samples' thermal stabilities were then analyzed using TGA/DTG and high-temperature PXRD. The TGA/DTG curves (Figure S3.1, Supporting Information) show that thermal decomposition starts in the 350–400 °C range. High temperature PXRD (Figure 1c,d) was then used to determine thermally induced loss of crystallinity, with NICS-21 retaining crystallinity up to 250 °C and NICS-22 up to 300 °C in air. Amorphization was observed after loss of crystallinity, which was followed by thermal decomposition and formation of NiO.

The prepared samples were activated to remove solvents and possible remains of reactants from pores, and N₂ isotherms (Figure 1e,f) were collected to determine S_{BET} , V_{micro} , and V_{total} (Table 1). The results show comparable S_{BET} determined for both samples as for their closest Zn counterparts, namely ZIF-90 and ZIF-93/94. The significantly lower surface area of NICS-22 (663 m² g⁻¹) compared to NICS-21 (1230 m² g⁻¹) is in accordance with the differences in the measured microporous pore volumes (Table 1) and the theoretical surface area (CCDC pore analyzer, from ED CIF structures NICS-21 1750 m² g⁻¹ and NICS-22 500 m² g⁻¹). The difference is first due to the presence of a bulkier ligand in NICS-22, if compared to NICS-21, which reduces the micropore volume. It is also noted that a similar trend in reduction of surface area between RHO and SOD topology was observed in the zinc(4-methyl-5-carboxaldehydeimidazolate)₂ isorecticular frameworks ZIF-94(SOD) and ZIF-93(RHO).

The CO₂, N₂, and CH₄ isotherms of both samples were then measured at 25 °C (Figure S4.1, Supporting Information) to assess basic gas capture behavior (Table 1). Of interest is the high CO₂/N₂ selectivity of both materials in the low-pressure region, which slowly decreases (Figure S4.2, Supporting Information) at higher relative pressures. Selectivity for CO₂/CH₄ remains mostly constant for both samples in the whole pressure range, with a drop in selectivity at higher relative pressures. NICS-22 shows a high selectivity for CO₂ at 50 mbar, which is in line with the inflection point observed in the adsorption isotherm in the 50–100 mbar pressure region.

NICS-21, while exhibiting the same linear isotherm, has a CO₂ uptake around 40% lower than that of its Zn analogue with the same ligand, ZIF-90,^[34] and about 20% lower than its topological analogue ZIF-93,^[35] which could be explained by the reduction of statistical interactions between the properly oriented dipoles

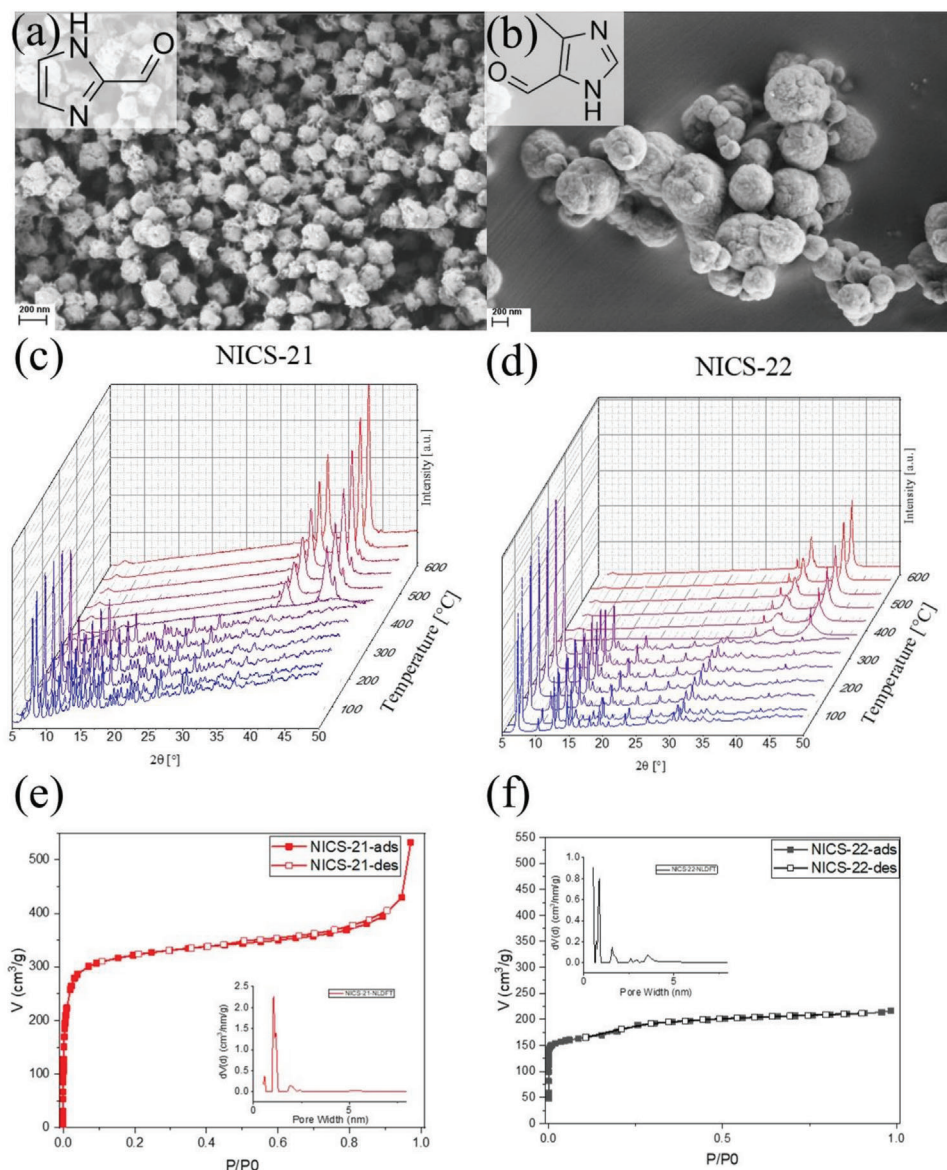


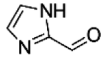
Figure 1. a–d) SEM and ligand structure of prepared NICS-21 (a) and NICS-22 (b), high temperature PXRD of NICS-21 (c) and NICS-22 (d). e, f) N_2 physisorption isotherms with NLDFT pore size distribution inserts for NICS-21 (e) and NICS-22 (f).

of the aldehyde group and CO_2 . This reduction is caused by the rigidity of the coordinated aldehydes and subsequent restrictions of C–C bond rotations within the cages. Potential increase of uptake due to the increase of the dipole moment of the aldehyde^[36] from coordination to Ni^{2+} is largely negated by the larger pore size, as that of ZIF-90.

NICS-22 exhibits the same Langmuir type isotherm as its closest topological and ligand-type Zn analogue, ZIF-94, but with a 23% higher uptake at 1 bar and 25 °C, that is, 2.8 $mmol\ g^{-1}$ compared to ZIF-94s 2.3 $mmol\ g^{-1}$.^[37] This improved CO_2 sorption performance could potentially be due to the slightly higher surface area and larger pore volume of the prepared NICS-22, as well as a potential increase in interaction strength through polarized Ni-coordinated aldehyde group.^[36]

Water isotherms were collected to investigate the behavior of frameworks in humid environments (Figure S4.3, Supporting Information). NICS-21's water isotherm exhibits a sharp inflection point at around 50% relative humidity, where the uptake jumps from 2 $mmol\ g^{-1}$ at 50% RH to 20 $mmol\ g^{-1}$ at 55% RH with a final uptake of 24.5 $mmol\ g^{-1}$ at 90% RH exhibiting no hysteresis and no changes in crystallinity of the sample after water sorption. NICS-22 water isotherm, on the other hand, has a very small inflection point at around 30% RH with a final uptake of 8.97 $mmol\ g^{-1}$ and with a pronounced hysteresis. The lower uptake is a consequence of the presence of methyl group on the ligand, which usually adds to the reduction of water uptake (enhanced hydrophobicity) and/or to the limited diffusion through narrower pores. Despite exhibiting a large hysteresis, amorphization

Table 1. Textural properties and sorption performance of NICS-21 and NICS-22, and their closest Zn counterparts with regard to type of ligand and framework topology.

Material	NICS-21	ZIF-90	NICS-22	ZIF-93	ZIF-94
					
Topology	RHO	SOD	SOD	RHO	SOD
S_{BET} [m ² g ⁻¹]	1230	1136 ^[38]	663	882 ^[39]	602 ^[39]
V_{micro} [mL g ⁻¹]	0.37	0.31 ^[38]	0.11	n.a.	n.a.
V_{total} [mL g ⁻¹]	0.84	0.51 ^[38]	0.34	0.42 ^[39]	0.29 ^[39]
CO ₂ uptake ^{a)} [mmol g ⁻¹]	1.11	1.95 ^[34] (2.03 ^{d)})	2.82	1.4 ^[35]	2.3 ^[37]
CO ₂ /N ₂ selectivity ^{b)}	17	23.6 ^[34] (17.8 ^{d)})	13	/	/
CO ₂ /CH ₄ selectivity ^{b)}	3.2	11.3 (6.8 ^{d)})	2.2	/	/
Water uptake ^{c)} [mmol g ⁻¹]	24.5	/	8.97	/	/
ρ [g mL ⁻¹]	0.780 ^{e)}	0.988 ^[39]	1.114 ^{e)}	0.991 ^[39]	1.204 ^[39]

^{a)} at 25 °C and 1 bar; ^{b)} ex situ selectivity calculated by $P_{\text{CO}_2}/P_{\text{X}}$ at 1 bar; ^{c)} 30 °C 0.9 P/P₀; ^{d)} sample from^[38] measured at the same conditions as NICS-21 and NICS-22; ^{e)} calculated density from structural data (CIF).

of the NICS-22 framework was not observed (Figure S2.3, Supporting Information).

2.2. Solving the Crystal Structure

Due to the small particle size, 3D electron diffraction (3D ED)^[40,41] was used to determine the structures of NICS-21 and NICS-22 (S5.3, Supporting Information), as both phases are acquired as nano-sized crystals. However, due to the high degree of agglomeration in the samples prepared initially, samples for 3D ED measurements were prepared using slightly modified synthesis procedures (S5.1 and S5.2, Supporting Information). The electron diffraction data was used to obtain crystal structure models and structure refinement for both NICS-21 and NICS-22 products (S5.3, Supporting Information). The refined structures coincide with the bulk samples (whole batches) with no indicated impurities, as demonstrated by the comparison of simulated and measured PXRD (Figure 2f,g).

The coordination environment around the metal centers in the nickel-based imidazolate structures of NICS-21 and NICS-22 is similar, with isolated nickel(II) cations coordinated to four imidazole ligands. Two ligands connect the cations through azolate nitrogen atoms in a bridging mode, while the remaining two ligands are coordinated in a chelating manner through additional carbonyl oxygen atoms originating from aldehyde functional groups. FTIR spectra of the prepared materials were collected (Figure S2.5, Supporting Information), and the coordination of the aldehyde oxygen further confirmed by the lack of the aldehyde C=O stretching vibration bands which would be expected at around (1750 cm⁻¹). This configuration of ligand coordination leads to a distorted octahedral environment around the nickel(II) cations (Figure 2c). The structures of NICS-21 and NICS-22 have zeolitic RHO and SOD framework topologies, respectively.

The changes and uniqueness of sixfold metal coordination result in slight deformations of RHO and SOD topologies when compared to the Zn-based frameworks with fourfold coordination. While the mean N–Ni–N angle values of 97.6° for NICS-21

and 96.9° for NICS-22, significantly deviate from the tetrahedral angle (109.5°) observed in Zn-based ZIF topological analogues, they still fall within the observed distribution of tetrahedral angles in transition metal 3D imidazolates in the CCDC 3D MOF subset.^[42] Although distorted, NICS-21 with RHO topology exhibits characteristic LTA cages with a diameter of 9.5 Å, accessible via elliptical-shaped eight-member rings with limiting openings of 4.0 Å (Figure 2a), estimated from the van der Waals radii of atoms. NICS-22 with SOD topology forms sodalite cages of 5.8 Å. However, the six-membered ring apertures enabling access to the cages have similar dimension to those of NICS-21 (4.1 Å).

2.3. Test of Catalytic Activity in Suzuki–Miyaura Reaction

We tested the prepared nickel ZIFs in the Suzuki–Miyaura (SM) cross-coupling reaction, where the coupling partners are boronic acids and organohalides (Figure 3 and S6, Supporting Information). The obtained results indicate that both NICS-21 and NICS-22 are suitable as catalysts for the reaction studied, and are interesting materials for further optimizations. By using 10 mol% of either ZIF with respect to the aryl halide substrate (which corresponds to about 10 mol% Ni with respect to the aryl halide), we were able to couple aryl iodides and aryl bromide with aryl boronic acids bearing substituents (H, OMe, and Cl) with different electronic properties in the para position (Figure 3). Similarly, the reaction worked with 4-iodotoluene, 4'-iodoacetophenone, and 4-iodo-1-indanone as substrates, as well as with 4-bromotoluene, showing the potential of the reaction for aryl bromides as well. Both materials proved to be suitable for effectively catalyzing the reaction, which was carried out in dioxane as a solvent at 100 °C in the presence of anhydrous K₃PO₄ as an additive for the activation of the boronic acid. The products were formed in 38–98% conversions as indicated by ¹H NMR using 1,3,5-trimethoxybenzene as an internal standard, and isolated in 38–74% yields (Figure 3).

The solid filtrate of both frameworks after the coupling of 4-iodotoluene and phenylboronic acid was analyzed with PXRD

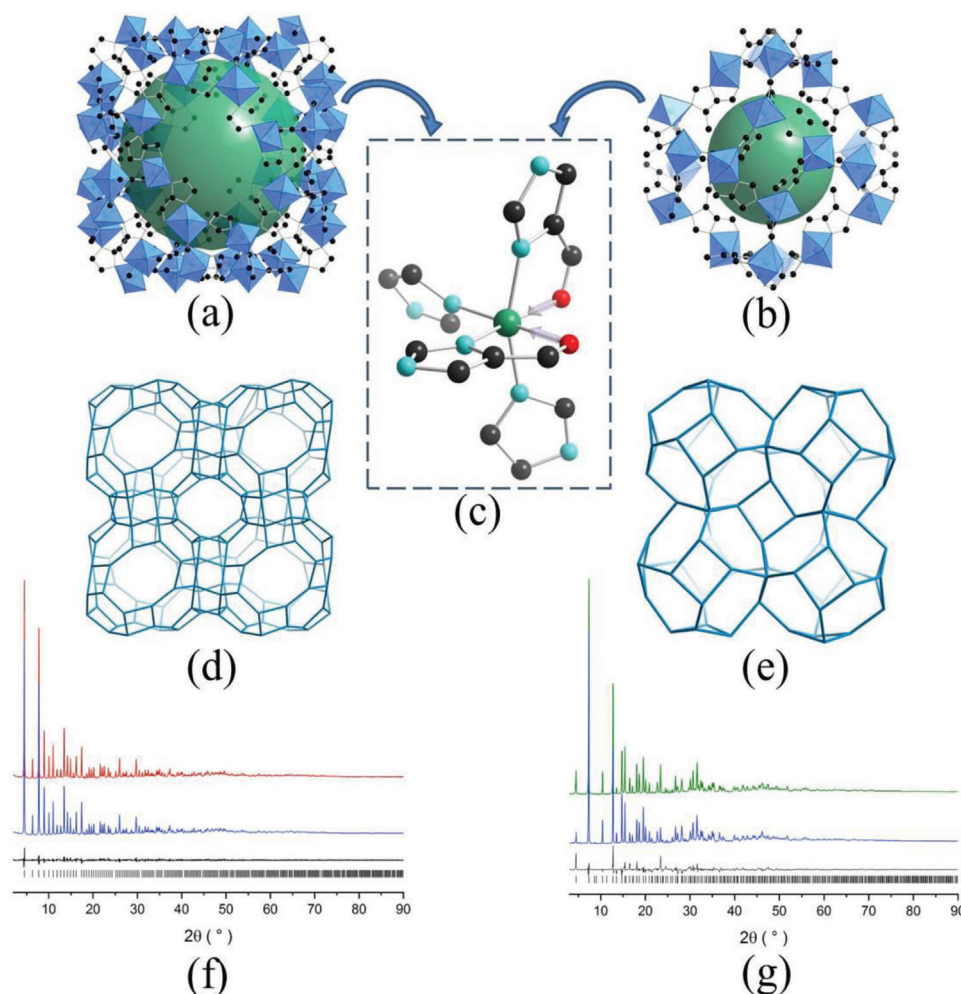


Figure 2. a) Representation of NICS-21 structure containing LTA cage and b) NICS-22 structure containing SOD cage with pore sizes of 9.5 and 5.8 Å, respectively, indicated by green balls. c) The sixfold coordination environment of nickel(II) centers in NICS-22 representative of both structures (methyl group from 4-methyl-5-imidazolecarboxaldehyde and hydrogen atoms from both ligands are omitted for clarity) shown as blue octahedra in (a) and (b), is formed from the four azolate nitrogen atoms (light blue balls) and two carbonyl oxygen atoms (red balls) originating from aldehyde functional groups on imidazoles. d,e) NICS-21 and NICS-22 exhibit distorted RHO and SOD framework topologies, respectively. XRD patterns of the refined f) NICS-21 and g) NICS-22 structures: experimental data (red and green lines), calculated diffractograms (blue line), differential plots (black line), and calculated reflection positions (black ticks).

(Figure S2.4, Supporting Information) to check for the retention of the crystallinity of the ZIFs after one and three runs of reactions. In the first attempt, no diffraction peak belonging to the starting frameworks was observed in the filtrate for either material. On the other hand, the reusability test revealed that the conversion to the expected 4-methyl-1,1'-biphenyl product was, in the case of NICS-21, similar for all three runs, that is, 64%, 54%, and 67% for the first, second, and third run, respectively. These results for the NICS-21 catalyst led us to retest the solid filtrate with PXRD, but this time the filtrate was immediately washed with water and ethyl acetate.

The PXRD (Figure S2.4, Supporting Information) of the washed filtrate now showed that the framework retains its structure after SM, with high crystallinity still observed, compared to the sample that was left as it was after filtration for multiple days before PXRD analysis. The exhibited stability of the material and its performance show a tremendous potential for

NICS-21 as a heterogeneous catalyst for SM reactions, with the caveat of proper washing of the catalyst after the reaction when not used for the following cycles right away. Interestingly, NICS-22 did not exhibit the same catalytic performance or the same cycling stability, that is, 52%, 25%, and 2% for the first, second, and third run, respectively, and it also amorphizes after the coupling test, as determined by the PXRD analysis. The origin of the differences in stability and performance between NICS-21 and NICS-22 in the SM cross-coupling reaction could potentially be due to the strain exhibited on the smaller voids of NICS-22 during the catalytic cycle or, in the case of 2-aldehyde group, easier ligand displacement and recombination when compared to the 4-aldehyde group on the ligands. Furthermore, the methyl group has an electron-donating effect, so the imidazole ring in NICS-22 is more electron-rich, which may also contribute to the structure and activity of NICS-22.

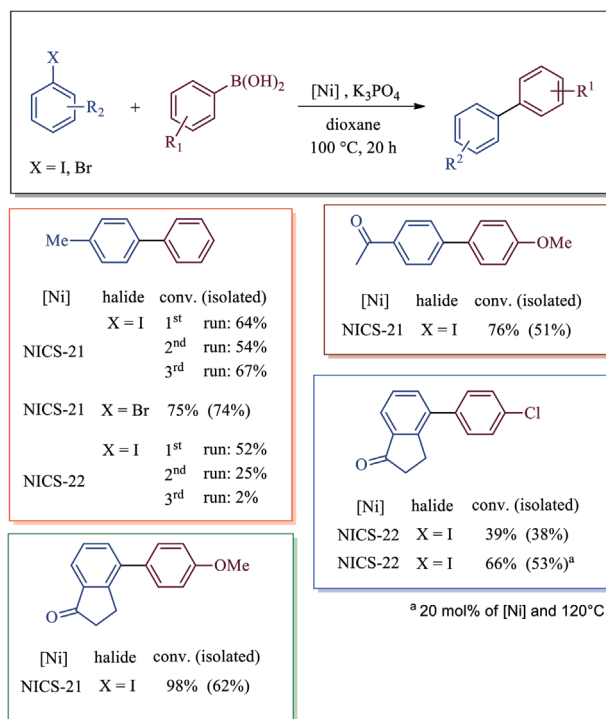


Figure 3. Heterogeneous Ni-ZIF catalyzed Suzuki–Miyaura cross-coupling reaction conditions and products obtained from aryl iodide and aryl bromide (blue) coupling with aryl boronic acids (purple) bearing various substituents (H, OMe, and Cl) with varying electronic properties. The scope of the heterogeneous catalysts with 10 mol% Ni is shown with respect to the aryl halide and 100 °C. The scheme shows the percentage of conversions and isolated materials (yields) in one run and, for one coupling reaction (4-iodotoluene and phenylboronic acid), in three consecutive runs.

3. Conclusion

Herein, we report the successful syntheses of the first pure nickel ZIFs with zeolitic RHO (NICS-21) and SOD (NICS-22) topologies. The hypothesis that linkers with additional functional groups that have the ability to coordinate to Ni²⁺ would complete nickel coordination octahedra and stabilize the framework was tested and confirmed. With future work on extending carboxyl-functionalized linkers to other coordinating functional groups that would allow the metal to stabilize in its preferred coordination state, we could possibly further expand the range of potential ZIF forming metal nodes. Both materials under investigation exhibit high thermal stability and permanent porosity, with comparable S_{BET} and CO₂ uptakes to their closest Zn analogues. The prepared materials were then successfully used as heterogeneous catalysts in Suzuki–Miyaura coupling reactions, showing promising activity for both materials and, in the case of NICS-21, reusability as well. Moreover, an important advantage of the developed Ni-based ZIFs lies in the ease of their synthesis and the conditions that they require to be catalytically active, that is, our catalysts allow for the preparation of potentially high-value precursors and intermediates with high yields under mild conditions in selected types of Ni-catalyzed transformations. Furthermore, NICS-22's high CO₂ uptake and NICS-21's high water up-

take could potentially allow for additional investigation into sorption applications.

Supporting Information

Supporting Information is available from the Wiley Online Library or from the author.

Acknowledgements

A.Š., M.M., and N.Z.L. acknowledge financial support from the Slovenian Research Agency (Research programme P1-0021; A.Š. acknowledges a Young Researcher Grant). A.M. acknowledges financial support from the Slovenian Research Agency (Research programme P1-0175). D.J. and M.G. acknowledge financial support from the Slovenian Research Agency (N1-0179, P1-0230; D.J. acknowledges a Young Researcher Grant) and the support of the Centre for Research Infrastructure at the University of Ljubljana, Faculty of Chemistry and Chemical Technology, which is part of the Network of Research and Infrastructural Centres UL (MRIC UL), and is financially supported by the Slovenian Research Agency (Infrastructure programme No. I0-0022). E.S.G. acknowledges support from the Swedish Research Council (registration number 2022–06178). The authors would like to thank Prof. Jože Grdadolnik for FTIR measurements, Mojca Opresnik for SEM/EDX measurements, and Edi Kranjc for XRD measurements. The authors thank Dr. Felix Hennersdorf from Rigaku Europe SE for providing the opportunity to make diffraction measurements of NICS-22 on the electron diffractometer XtaLAB Synergy-ED with the Hypix3000-ED detector.

Conflict of Interest

The authors declare no conflict of interest.

Data Availability Statement

The data that support the findings of this study are available in the supplementary material of this article.

Keywords

heterogeneous catalysis, nickel catalysis, Suzuki–Miyaura cross coupling, zeolitic imidazolate frameworks

Received: June 23, 2023
Revised: September 20, 2023
Published online: October 5, 2023

- [1] H. Lin, Y. Yang, Y.-C. Hsu, J. Zhang, C. Welton, I. Afolabi, M. Loo, H.-C. Zhou, *Adv. Mater.* **2023**, 2209073, <https://doi.org/10.1002/adma.202209073>.
- [2] M. Younas, M. Rezakazemi, M. Daud, M. B. Wazir, S. Ahmad, N. Ullah, Inamuddin, S. Ramakrishna, *Prog. Energy Combust. Sci.* **2020**, *80*, 100849.
- [3] A. Dhakshinamoorthy, A. M. Asiri, H. Garcia, *Chem. Soc. Rev.* **2015**, *44*, 1922.
- [4] H. Wang, X. Pei, M. J. Kalmutzki, J. Yang, O. M. Yaghi, *Acc. Chem. Res.* **2022**, *6*, 1c00740.
- [5] A. Phan, C. J. Doonan, F. J. Uribe-Romo, C. B. Knobler, M. Okeeffe, O. M. Yaghi, *Acc. Chem. Res.* **2010**, *43*, 58.

- [6] G. Jiang, V. Bon, F. Xu, B. Garai, E. Zhang, I. Senkowska, S. Poetke, F. Hippauf, S. Hausdorf, S. Paasch, E. Brunner, H. Wang, S. Kaskel, *Dalton Trans.* **2021**, 50, 7933.
- [7] J. López-Cabrelles, J. Romero, G. Abellán, M. Giménez-Marqués, M. Palomino, S. Valencia, F. Rey, G. M. Espallargas, *J. Am. Chem. Soc.* **2019**, 141, 7173.
- [8] K. Kadota, E. Sivaniah, S. Bureekaew, S. Kitagawa, S. Horike, *Inorg. Chem.* **2017**, 56, 8744.
- [9] S. Horike, K. Kadota, T. Itakura, M. Inukai, S. Kitagawa, *Dalton Trans.* **2015**, 44, 15107.
- [10] Y. Wang, L. Yao, S. Wang, D. Mao, C. Hu, *Fuel Process. Technol.* **2018**, 169, 199.
- [11] A. N. Mlinar, B. K. Keitz, D. Gygi, E. D. Bloch, J. R. Long, A. T. Bell, *ACS Catal.* **2014**, 4, 717.
- [12] H. Olivier-Bourbigou, P. A. R. Breuil, L. Magna, T. Michel, M. F. E. Pastor, D. Delcroix, *Chem. Rev.* **2020**, 120, 7919.
- [13] N. Hongloi, P. Prapainainar, C. Prapainainar, *Mol. Catal.* **2022**, 523, 111696.
- [14] N. A. Sholeha, H. Holilah, H. Bahruji, A. Ayub, N. Widiastuti, R. Ediaty, A. A. Jalil, M. Ulfa, N. Masruchin, R. E. Nugraha, D. Prasetyoko, *S. Afr. J. Chem. Eng.* **2023**, 44, 14.
- [15] R. Pothu, R. Bolagam, Q.-H. Wang, W. Ni, J.-F. Cai, X.-X. Peng, Y.-Z. Feng, J.-M. Ma, *Rare Met.* **2021**, 40, 353.
- [16] D. Zhou, X. Guo, Q. Zhang, Y. Shi, H. Zhang, C. Yu, H. Pang, D. Zhou, X. Guo, Q. Zhang, Y. Shi, H. Zhang, H. Pang, C. Yu, *Adv. Funct. Mater.* **2022**, 32, 2107928.
- [17] F. Ma, Y. Zhao, J. Li, X. Zhang, H. Gu, J. You, *J. Energy. Chem.* **2021**, 52, 393.
- [18] S. Kousik, S. Velmathi, *Chem. - Eur. J.* **2019**, 25, 16451.
- [19] S. Bachmann, J. A. Van Bokhoven, K. Püntener, M. Ranocchiari, F. Hoffmann, D. Cartagenova, *Chimia* **2021**, 75, 972.
- [20] J. R. Ludwig, C. S. Schindler, *Chem* **2017**, 2, 313.
- [21] V. P. Ananikov, *ACS Catal.* **2015**, 5, 1964.
- [22] R. Ramírez-Contreras, B. Morandi, G. Jiang, V. Bon, F. Xu, B. Garai, E. Zhang, I. Senkowska, S. Poetke, F. Hippauf, S. Hausdorf, S. Paasch, E. Brunner, H. Wang, S. Kaskel, *Non-Noble Met. Catal.* **2018**, 127, <https://doi.org/10.1002/9783527699087>.
- [23] P. Elumalai, H. Mamlouk, W. Yiming, L. Feng, S. Yuan, H.-C. Zhou, S. T. Madrahimov, *ACS Appl. Mater. Interfaces* **2018**, 10, 41431.
- [24] R. A. Maia, F. Berg, V. Ritleng, B. Louis, P. M. Esteves, *Chem. - Eur. J.* **2020**, 26, 2051.
- [25] D. Canseco-Gonzalez, A. Gniewek, M. Szulmanowicz, H. Müller-Bunz, A. M. Trzeciak, M. Albrecht, *Chem. - Eur. J.* **2012**, 18, 6055.
- [26] R. Li, X. Ren, H. Ma, X. Feng, Z. Lin, X. Li, C. Hu, B. Wang, *J. Mater. Chem. A* **2014**, 2, 5724.
- [27] C. Chen, M. R. Alalouni, X. Dong, Z. Cao, Q. Cheng, L. Zheng, L. Meng, C. Guan, L. Liu, E. Abou-Hamad, J. Wang, Z. Shi, K.-W. Huang, L. Cavallo, Y. Han, *J. Am. Chem. Soc.* **2021**, 143, 7144.
- [28] X. Ding, H. Liu, J. Chen, M. Wen, G. Li, T. An, H. Zhao, *Nanoscale* **2020**, 12, 9462.
- [29] A. M. Kale, R. Manikandan, C. J. Raj, A. D. Savariraj, C. Voz, B. C. Kim, *Mater. Today Energy* **2021**, 21, 100736.
- [30] L. Rulišek, J. Vondrášek, *J. Inorg. Biochem.* **1998**, 71, 115.
- [31] C. Baerlocher, L. B. McCusker, Database of Zeolite Structures, <http://www.iza-structure.org/databases/> (accessed: May 2023).
- [32] M. T. Wharmby, S. Henke, T. D. Bennett, S. R. Bajpe, I. Schwedler, S. P. Thompson, F. Gozzo, P. Simoncic, C. Mellot-Draznieks, H. Tao, Y. Yue, A. K. Cheetham, *Angew. Chem.* **2015**, 127, 6547.
- [33] X. Li, Z. Li, L. Lu, L. Huang, L. Xiang, J. Shen, S. Liu, D. R. Xiao, *Chem. - Eur. J.* **2017**, 23, 10638.
- [34] M. Usman, M. Y. Khan, T. Anjum, A. L. Khan, B. Hoque, A. Helal, A. S. Hakeem, B. A. Al-Maythalony, *Membranes* **2022**, 12, 1055.
- [35] E. V. Ramos-Fernandez, A. Grau-Atienza, D. Farrusseng, S. Aguado, *J. Mater. Chem. A* **2018**, 6, 5598.
- [36] F. Mohajer, M. N. Shahrak, *Heat Mass Transfer* **2019**, 55, 2017.
- [37] A. Sabetghadam, X. Liu, M. Benzaqui, E. Gkaniatsou, A. Orsi, M. M. Lozinska, C. Sicard, T. Johnson, N. Steunou, P. A. Wright, C. Serre, J. Gascon, F. Kapteijn, *Chem. - Eur. J.* **2018**, 24, 7949.
- [38] A. Škrjanc, C. Byrne, N. Zabukovec Logar, *Molecules* **2021**, 26, 1573.
- [39] M. Gao, J. Wang, Z. Rong, Q. Shi, J. Dong, *RSC Adv.* **2018**, 8, 39627.
- [40] Z. Huang, E. S. Grape, J. Li, A. K. Inge, X. Zou, *Coord. Chem. Rev.* **2021**, 427, 213583.
- [41] M. Gemmi, E. Mugnaioli, T. E. Gorelik, U. Kolb, L. Palatinus, P. Boullay, S. Hovmöller, J. P. Abrahams, *ACS Cent. Sci.* **2019**, 5, 1315.
- [42] C. R. Groom, I. J. Bruno, M. P. Lightfoot, S. C. Ward, *Acta Crystallogr., Sect. B: Struct. Sci., Cryst. Eng. Mater.* **2016**, 72, 171.